tvst

Special Issue

Inhibition of Sema-3A Promotes Cell Migration, Axonal Growth, and Retinal Ganglion Cell Survival

Anat Nitzan[1], Miriam Corredor-Sanchez[2], Ronit Galron[1], Limor Nahary[3], Mary Safrin[4], Marina Bruzel[4], Alejandra Moure[2], Roman Bonet[2], Yolanda Pérez[2], Jordi Bujons[2], Enriqueta Vallejo-Yague[5], Hagit Sacks[6], Michael Burnet[5], Ignacio Alfonso[2], Angel Messeguer[2], Itai Benhar[3], Ari Barzilai[1,7,*], and Arieh S. Solomon[4,7,*]

[1] Department of Neurobiology, George S. Wise, Faculty of Life Sciences, Tel Aviv University, Tel Aviv, Israel
[2] Department of Biological Chemistry, Institute of Advanced Chemistry of Catalonia, IQAC-CSIC, Barcelona, Spain
[3] The Shmunis School of Biomedicine and Cancer Research, George S. Wise, Faculty of Life Sciences, Tel Aviv University, Tel Aviv, Israel
[4] Goldschleger Eye Research Institute, Sheba Medical Center, Tel Aviv University Tel Aviv, Israel
[5] Synovo GmbH, Tübingen, Germany
[6] Nicast Ltd., Global Park, Lod, Israel
[7] Sagol School of Neuroscience, Tel Aviv University, Tel Aviv, Israel

Correspondence: Arieh S. Solomon, FARVO, Goldschleger Eye Research Institute, Sackler Faculty of Medicine, Tel Aviv University, Sheba Medical Center 62126, Israel.
e-mail: asolomon@post.tau.ac.il

Received: March 2, 2021
Accepted: September 9, 2021
Published: November 24, 2021

Keywords: Semaphorin 3A; retinal ganglion cells; antibody; small molecule

Citation: Nitzan A, Corredor-Sanchez M, Galron R, Nahary L, Safrin M, Bruzel M, Moure A, Bonet R, Pérez Y, Bujons J, Vallejo-Yague E, Sacks H, Burnet M, Alfonso I, Messeguer A, Benhar I, Barzilai A, Solomon AS. Inhibition of Sema-3A promotes cell migration, axonal growth, and retinal ganglion cell survival. Transl Vis Sci Technol. 2021;10(10):16, https://doi.org/10.1167/tvst.10.10.16

Purpose: Semaphorin 3A (Sema-3A) is a secreted protein that deflects axons from inappropriate regions and induces neuronal cell death. Intravitreal application of polyclonal antibodies against Sema-3A prevents loss of retinal ganglion cells ensuing from axotomy of optic nerves. This suggested a therapeutic approach for neuroprotection via inhibition of the Sema-3A pathway.

Methods: To develop potent and specific Sema-3A antagonists, we isolated monoclonal anti-Sema-3A antibodies from a human antibody phage display library and optimized low-molecular weight Sema-3A signaling inhibitors. The best inhibitors were identified using in vitro scratch assays and semiquantitative repulsion assays.

Results: A therapeutic approach for neuroprotection must have a long duration of action. Therefore, antibodies and low-molecular weight inhibitors were formulated in extruded implants to allow controlled and prolonged release. Following release from the implants, Sema-3A inhibitors antagonized Sema-3A effects in scratch and repulsion assays and protected retinal ganglion cells in animal models of optic nerve injury, retinal ischemia, and glaucoma.

Conclusions and Translational Relevance: Collectively, our findings indicate that the identified Sema-3A inhibitors should be further evaluated as therapeutic candidates for the treatment of Sema-3A-driven central nervous system degenerative processes.

Introduction

Semaphorins are secreted and membrane-bound proteins that primarily act as axonal growth cone guidance molecules. They relay short-range inhibitory signals through multimeric receptor complexes to deflect axons from inappropriate regions. These cues are especially important in neural system development. The major class of receptors for semaphorins are the plexins. Every semaphorin includes a region of about 500 amino acids called the sema domain.[1]

There are eight major classes of semaphorins. The first 7 are identified by number, from class 1 to class 7. The eighth group is class V, where V stands for virus. Classes 3, 4, 6, and 7 are specific to vertebrates,

classes 1 and 2 are found only in invertebrates, and class 5 is found in both. Each class of semaphorin has many subgroups. Semaphorins were first discovered in the context of axon guidance in the limb buds of grasshoppers in 1992,[2] but, since then, diverse roles for semaphorins have been identified. They not only guide axons in development, but also have major roles in immune function (classes 4, 6, and 7)[3] and the development of bones.[4]

One of the most versatile semaphorin classes is class 3. Each one of the class 3 semaphorins is expressed in a different region of the body during development. Whereas some encourage the growth of axons, others cause the inhibition of this growth. Semaphorin 3A (Sema-3A) repels axons from the dorsal root ganglia,[5] sympathetic ganglia,[6] facial nerves,[7] vagal nerves,[8] olfactory-sensory nerves,[9] cortical nerves,[10] hippocampal nerves,[11] and cerebellar nerves.[12] Sema-3A exerts its biological function through the activation of neuropilin-plexin receptor complexes.[13–15]

In addition to its role as axonal guidance molecule during development, Sema-3A levels are altered after central nervous system (CNS) injury in mammals[16–19] and fish.[20] Using in vitro experiments, we identified Sema-3A as a death-inducing factor for sympathetic neurons.[21] Expression of class 3 semaphorins is induced for a short period of time after complete axotomy and is correlated with retinal ganglion cell (RGC) death. Neutralization of Sema-3A activity markedly reduces the death of RGCs following optic nerve axotomy in adult rats.[22] In contrast to acute optic nerve injury, which results in a brief elevation in Sema-3A levels, a prolonged increase in levels of Sema-3A is detected in glaucomatous rabbits. Immunohistochemical analysis revealed that Sema-3A expression is upregulated specifically in the ganglion cell layer, which is a structure that is highly affected in glaucoma.[23] Upregulation of Sema-3A is also observed following retinal detachment.[24] In contrast to mammals, Sema-3A is not elevated upon nerve injury in goldfish. There is a decrease of about 60% in Sema-3A levels in the goldfish retina at an early stage after optic nerve injury but almost no change in Sema-3A levels in the injured optic nerve. Intravitreal injection of Sema-3A into a goldfish eye shortly after optic nerve injury reduces survival of RGCs, axonal growth, and clearance of myelin debris from the lesion site by macrophages.[25] These data suggest that, whereas Sema-3A hinders regeneration in the mammalian eye following injury or disease, the goldfish eye, which is known to be more adapted to regeneration after injury, clearly circumvents that hindrance by transient downregulation of Sema-3A expression.

Although low levels of Sema-3A seem to be beneficial, its excess is detrimental. Nijmegen breakage syndrome is a genomic instability disorder that severely affects the CNS. Conditional disruption of the *Nbs1* gene in the mouse CNS leads to dramatic CNS degeneration that is associated with increased levels Sema-3A and its receptor neuropilin-1.[26] Collectively, these findings show that Sema-3A is involved in response to injury and stress and that its presence is associated with loss of neuronal tissue. The complexes of semaphorins, neuropilins, and plexins are thus potential targets for treatment of various diseases.[27]

Here, we used several in vitro assays to test the potency of Sema-3A inhibitors. We found that a small-molecule Sema-3A inhibitor, CSIC002, and a function-blocking anti-Sema-3A antibody Fab 3H4 inhibited the deleterious effects of Sema-3A. We also showed that the potency of the Sema-3A inhibitors was not diminished when formulated in polycaprolactone (PCL) implants. Most importantly, the Sema-3A inhibitors protected RGCs from insults, such as optic nerve injury, acutely induced glaucoma, and retinal ischemia in animal models.

Methods

Synthesis of CSIC002

General. Reagents and solvents were purchased from commercial suppliers (Aldrich, Fluka, or Merck) and were used without further purification. Flash chromatography purifications were performed on a BioTage instrument. Reversed-phase purifications were performed using KP-C18-HS cartridges, and normal-phase purifications were performed using KP-Sil cartridges. The nuclear magnetic resonance (NMR) spectroscopic experiments were carried out on a Varian MERCURY 400 spectrometer (400 MHz for ^{1}H and 100 MHz for ^{13}C) at 298 K. Chemical shifts are given in ppm (δ) relative to internal transcranial magnetic stimulation (TMS), and coupling constants (J) are reported in Hertz (Hz). Analytical reversed phase high-performance liquid chromatography (RP-HPLC) was performed with a Hewlett Packard Series 1100 (UV detector 1315A) modular system using an X-Terra C_{18} (15 × 0.46 cm, 5 μm). CH_3CN-H_2O mixtures containing 0.1% TFA at 1 mL/min were used as mobile phase and monitoring wavelength was set at 220 nm. The gradient used was from 5% to 100% CH_3CN in 20 minutes. High-resolution mass spectra (HRMS) were acquired on an Acquity UPLC System and a LCT PremierTM XE Benchtop orthogonal

acceleration time-of-flight (Waters Corporation) equipped with an electrospray ionization source.

***Tert*-butyl *N*-[2-(diethylamino)ethyl]glycinate (1)**. To a solution of *N*,*N*-diethylethylenediamine (3.6 mL, 25.8 mmol) and triethylamine (7.2 mL, 51.6 mmol) in 25 mL of THF, *tert*-butyl bromoacetate (3.8 mL, 25.8 mmol) was added at 0°C. The mixture was allowed to react overnight at room temperature. The solvent was evaporated to dryness, and the residue obtained was treated with water and extracted with DCM. The organic layer was washed with water, dried, and filtered. The solvent was eliminated. The ^{1}H-NMR spectrum showed a ratio 4.6:1 of monoalkylation to dialkylation products. The residue was distilled under vacuum to yield 2.9 g of *tert*-butyl *N*-[2-(diethylamino)ethyl]glycinate (85°C, 0.3 Torr, 49%). HRMS and NMR data are shown in the Supplementary section.

***Tert*-butyl *N*-benzyloxycarbonyl-*N*-[2-(diethylamino)ethyl]glycinate (2)**. Benzyl chloroformate (2.5 mL, 17.7 mmol) was added to a solution of *tert*-butyl *N*-[2-(diethylamino)ethyl]glycinate (3.7 g, 16.1 mmol) and K_2CO_3 (6.7 g, 48.3 mmol) in 32 mL of dioxane/H_2O (1:1) at 0°C. The mixture was allowed to react overnight at room temperature. The organic solvent was evaporated, and the residue was extracted with DCM (3 × 10 mL). The pooled organic fractions were filtered. The solvent was removed under reduced pressure, and the residue was purified by flash chromatography using DCM and MeOH as eluent (from 0% to 2% MeOH, DCM contained 1% Et_3N) to give 5.1 g of *tert*-butyl *N*-benzyloxycarbonyl-*N*-[2-(diethylamino)ethyl]glycinate (87% yield, room temperature for 12.9 minutes). HRMS and NMR data are shown in the Supplementary section.

***N*-benzyloxycarbonyl-*N*-[2-(diethylamino)ethyl]glycine hydrochloride (3)**. To 1.8 g of *tert*-butyl *N*-benzyloxycarbonyl-*N*-[2-(diethylamino)ethyl]glycinate (4.9 mmol) was added 6.0 ml of HCl/dioxane (4 M, 24.0 mmol), the mixture was allowed to react for 1 hour at 60°C (high-performance liquid chromatography [HPLC] control, room temperature for 10.6 minutes). The solvent was removed under reduced pressure to yield 1.6 g of *N*-benzyloxycarbonyl-*N*-[2-(diethylamino)ethyl]glycine hydrochloride (99% yield). It was used without further purification. HRMS and NMR data are shown in the Supplementary section.

***Tert*-butyl N-[(2-pyrrolidin-1-yl)ethyl]glycinate (4)**. To a mixture of 1-(2-aminoethyl)pyrrolidine (3.0 ml, 23.7 mmol) and K_2CO_3 (9.8 g, 71 mmol) in 25 mL of THF, *tert*-butyl bromoacetate (3.5 mL, 23.7 mmol) was added at 0°C. The mixture was allowed to react for 30 minutes at room temperature, was filtered, and the solvent was evaporated to dryness. The residue obtained was treated with water (20 mL) and extracted with DCM (25 mL), filtered, and dried. The ^{1}H-NMR spectrum showed a ratio 5.6:1 of monoalkylation product to dialkylation product. The residue was distilled under vacuum to yield 2.9 g of *tert*-butyl *N*-[(2-pyrrolidin-1-yl)ethyl]glycinate (85°C, 0.3 Torr, 54%). HRMS and NMR data are shown in the Supplementary section.

***Tert*-butyl-3-(2-pyrrolidin-1-yl)ethyl-6-benzyloxycarbonyl-9-diethyl-4-oxo-3,6,9-triazanonanoate (5)**. To a solution of *N*-benzyloxycarbonyl-*N*-[2-(diethylamino)ethyl]glycine hydrochloride (644 mg, 1.87 mmol) in 10.0 mL of anhydrous DCM were added Et_3N (340 µL, 2.43 mmol) and DCC (503 mg, 2.43 mmol). The mixture was stirred for 3 minutes at 60°C under microwave conditions, and *tert*-butyl *N*-[(2-pyrrolidin-1-yl)ethyl]glycinate (470 mg, 2.06 mmol) was added. The mixture was stirred under microwave conditions for 40 minutes at 60°C (HPLC control, room temperature for 10.7 minutes). The crude was filtered, and the solid washed with DCM and dried under vacuum. The residue was purified by reverse-phase chromatography using CH_3CN/H_2O as eluent (from 5% to 50% CH_3CN) to give 504.2 mg of *tert*-butyl 3-(2-pyrrolidin-1-yl)ethyl-6-benzyloxycarbonyl-9-diethyl-4-oxo-3,6,9-triazanonanoate (52% yield). HRMS and NMR data are shown in the Supplementary section.

Preparation of carboxylic acid 6. To 500 mg of *tert*-butyl 3-(2-pyrrolidin-1-yl)ethyl-6-benzyloxycarbonyl-9-diethyl-4-oxo-3,6,9-triazanonanoate (0.96 mmol) was added 2.2 mL of HCl/dioxane (4 M, 8.69 mmol), the mixture was allowed to react for 1 hour at 60°C (HPLC control, room temperature for 9.0 min). Solvent was removed under reduced pressure to obtain 515.4 g of 3-(2-pyrrolidin-1-yl)ethyl-6-benzylloxycarbonyl-9-diethyl-4-oxo-3,6,9-triazanonanoic acid dihydrochloride (99 % yield). It was used without further purification. HRMS and NMR data are shown in the Supplementary section.

[2-(1-Methylpyrrolidin-2-yl)ethylamino]acetamide (7). An aliquot of 2 mL of 2-(2-aminoethyl)-1-methylpyrrolidine (13.8 mmol) was dissolved in 75 mL of THF, and 5.7 g of K_2CO_3 (41.4 mmol) were added. The mixture was cooled to 0°C, and bromoacetamide (1.9 g, 13.8 mmol) was added slowly. The mixture was stirred for 2 hours at room temperature, filtered, and the THF was allowed to evaporate. The residue was distilled under vacuum to yield [2-(1-methylpyrrolidin-2-yl)ethylamino]acetamide (120°C, 0.3 Torr). HRMS and NMR data are shown in the Supplementary section.

3-[2-(1-Methylpyrrolidin-2-yl)ethyl]-6-(2-pyrrolidin-1-yl)ethyl-9-benzyloxycarbonyl-12-diethyl-4,7-dioxo-3,6,9,12-tetraazadodecancarboxamide (CSIC002). To a solution of 3-(2-pyrrolidin-1-yl)ethyl-6-benzylloxy carbonyl-9-diethyl-4-oxo-3,6,9-triazanonanoic acid dihydrochloride (290 mg, 0.54 mmol) in 4.0 mL of anhydrous DCM was added Et_3N (230 µL, 1.63 mmol) and DCC (145.7 mg, 0.71 mmol). The mixture was stirred 2 minutes at 45°C under microwave conditions, and [2-(1-methylpyrrolidin-2-yl)ethylamino]acetamide was added. The mixture was stirred under microwave conditions for 1.5 hours at 45°C (HPLC control, room temperature for 8.1 minutes). The crude was filtered, the solid was washed with DCM, and the solvent was removed under vacuum. The residue was purified by reverse-phase chromatography using CH_3CN/H_2O as eluent (from 0% to 40% CH_3CN) to give 78.4 mg of 3-[2-(1-methylpyrrolidin-2-yl)ethyl]-6-(2-pyrrolidin-1-yl)ethyl-9-benzyloxycarbonyl-12-diethyl-4,7-dioxo-3,6,9,12-tetraazadodecancarboxamide (23% yield). HRMS and NMR data are shown in the Supplementary section.

Isolation of Sema-3A-Specific Antibodies

Identification of Sema-3A-specific antibodies was carried out in two steps. The first step involved the identification of antigen-specific binders. At this step, the potential of the antibodies to modulate biological activities cannot be evaluated. Therefore, in the second step, the "hits" from step 1 were converted to soluble antibodies using either Fab or human IgG1 expression vectors. Fabs and IgGs were produced using the bacterial expression system "Inclonals."[32] The purified antibodies were evaluated for binding affinity and specificity by ELISA.

Isolation of Sema-3A-specific Antibodies by Phage Display

Sema-3A-specific antibodies were isolated from the Ronit 1 human antibody phage display library.[28] As bait for affinity selection, we used the 65-kDa, furin-cleaved extracellular domain of the human Sema-3A protein (residues 359–366), which contains the functional regions of Sema-3A[29]; this cleavage product is referred to as Sema-3A(65). Sema-3A(65) was purified from the conditioned medium of HEK293 cells transfected with a suitable expression vector[30] (kindly provided by Prof. Gera Neufeld, Technion, Israel). Affinity selection of the phage library was carried out essentially as described.[31] Because the Sema-3A antigen was only partially purified, the protocol was modified as follows: a single well of a 24-well tissue culture plate was coated with 1 mL of 5 µg/mL mouse monoclonal anti-Sema-3A[22] in phosphate-buffered saline (PBS). Library phages were mixed with Sema-3A, and the phage-Sema-3A complexes were captured on the immobilized monoclonal antibody. Phages that bound contaminating proteins in the Sema-3A fraction were not captured and were washed away. Three or four affinity selection cycles were carried out. In the odd numbered cycles, a "sandwich" capture was applied, and, in the even numbered cycles, phages were captured by Sema-3A coated directly onto wells. Phage enzyme-linked immunosorbent assay (ELISA) was used to identify Sema-3A binders.

Production of Recombinant Fab Antibodies for Evaluation in Bioassays

Phage-displayed single-chain Fvs (scFvs) were converted to soluble expression as Fabs in a process in which the VH and VL domains were made from synthetic genes optimized for expression in *E. coli*, appended with a C-terminal His tag fused to the Fd fragment of the heavy chain. The Fabs were produced by bacterial expression and refolded essentially, as described previously,[32] and purified with Ni-NTA metal-chelate chromatography (HisTrap columns, GE Healthcare). The Fabs were evaluated for Sema-3A binding affinity and specificity by ELISA. The Fabs were ranked according to manufacturability and apparent binding affinity to Sema-3A. The leading candidates were tested for inhibition of Sema-3A-mediated signaling.

Production of Full-Length Human IgG1 Antibodies Using Bacterial Expression

The Fabs described above were also produced as human IgG1 along with an isotype control antibody that binds streptavidin using a bacterial expression system.[32,33] IgGs produced in this manner are a-glycosylated, hence they do not activate complement nor do they engage immune effector cells (because they do not bind Fc gamma receptors). There is a concern that in a diseased eye, immune cells (primarily macrophages) invade and their activation by antibodies is to be avoided.

To produce IgGs, plasmids that carry the heavy and the light chains were introduced separately into *E. coli* cells, and expression was induced with IPTG. The heavy and light chains accumulated as insoluble inclusion bodies that were recovered and solubilized in 6 M guanidinium hydrochloride Tris buffer pH 8. The

solubilized inclusion bodies were mixed at a 1:2 heavy chain:light chain molar ratio, reduced using dithioerythritol, and refolded by rapid mixing into a refolding solution consisting of Tris, oxidized glutathione, and arginine. The samples were incubated at 10°C for 60 hours. The refolded IgG was then concentrated using a diafiltration device and buffer exchanged into 20 mM Tris-HCl, pH 7.0, 500 mM NaCl. The concentrated and refolded IgGs were loaded onto HiTrap MabSelect columns (GE Healthcare) and eluted using 0.1 M citric acid, pH 3.0. The eluted IgGs were neutralized with 1.5 M Tris-HCl, pH 8.5. To remove aggregates, the IgGs were separated on a 320-mL Hiprep Sephacryl 26/60 column (GE Healthcare). The monomeric IgGs were stored at −80°C.

Determination of Binding Affinities of IgGs and Fabs by ELISA

An ELISA plate was coated with 5 µg/mL Sema-3A and blocked with 3% skim milk in PBS. IgGs were tested in a 2-fold dilution series starting at a concentration of 1000 nM. Binding was detected using an HRP-conjugated goat-anti-human antibody (H+L; Jackson Immunoresearch Laboratories) diluted 5000-fold in PBST. Color reaction was carried out using the HRP substrate TMB. Color development was terminated after 20 minutes with 1 M H_2SO_4 and the plate was read at 450 nm.

Cell Morphology Assay

U87MG cells were seeded at 1×10^4 cells per well in 12-well plates, on cover slips without coating. The following day, the cells were exposed to different concentrations of Sema-3A (125 ng, 250 ng, 500 ng, and 750 ng) in serum-free medium. No Sema-3A was added to the wells that served as controls. After 35 minutes, cells were fixed with 4% PFA in PBS for 10 minutes, rinsed twice with PBS, incubated with a blocking solution (1% bovine serum albumin [BSA], 10% NGS and 0.25% Triton X-100 in PBS) for 1 hour, and stained either with rabbit anti-neuropilin-1 antibody (1:50; Santa Cruz Biotechnology, SC-5307) or with mouse monoclonal vinculin antibody 1:1000 (Sigma V9264) overnight at 4°C. The cells were then incubated with an Alexa fluor 488-conjugated goat anti-rabbit secondary antibody for 1 hour at room temperature followed by incubation with phalloidin-TRITC (1:200; Sigma) for 40 minutes. The cover slips were mounted on slides using Sigma mounting medium and viewed under a Zeiss LSM 510 confocal microscope.

Scratch Assay

U87MG cells were seeded on 12-well plates at 3×10^4 cells per well. After 2 days, a scratch was made in each well using a 200-µL pipet tip. Sema-3A (1 µg/mL) was incubated with 10 µg/mL of Fab 3H4 or 10 µM of CSIC002 or were vehicle treated for 30 minutes at room temperature. A mixture of Sema-3A and the inhibitor or vehicle was then added to the U87MG cells. After 24 hours at 37°C, the reaction was stopped by removing the medium and adding 4% PFA in PBS for 10 minutes. The cells were then stained with DAPI and images were taken with a fluorescence microscope. The number of cells in the scratch was quantified by using ImageJ software.

DRG Repulsion Assay

Fertilized chicken eggs were placed in an incubator at 37°C 12 days before the day of the experiment. HEK293-Sema-3A secreting cells (curtesy of the Neufeld laboratory) were thawed and seeded 5 days before the day of the experiment. After 48 hours, the cells were harvested and re-plated. One day prior to the day of the experiment, 12-well plates were coated with poly-D-lysine for 2 hours at room temperature. The plates were washed twice with sterile doubly distilled water and left to dry in the biosafety cabinet. When the plates were dry, ibidi 2-well culture inserts were positioned in the middle of each well. Sema-3A-secreting HEK293 cells were harvested, counted, and a solution of 3×10^5 cells/mL medium was prepared. This solution (70 µL) was added to each side of the inserts (a total of 140 µL per insert), and the plates were placed in the incubator overnight. On the day of the experiment, the wells were coated with 4 µg/mL of laminin all around the ibidi insert, but not inside it, and plates were incubated for 2 hours at room temperature. At the end of the 2 hours, laminin was removed from the plates, and they were left to dry in the biosafety cabinet. In the meantime, a fresh neurobasal medium (Gibco) containing 2% B27, 1% PSN, 1% l-glutamine, and 1% sodium pyruvate was prepared with 50 ng/µL of NGF (Peprotech). The dorsal root ganglions (DRGs) were dissected from between thoracic and upper lumbar regions of 12-day-old embryos and placed in a 35-mm dish with warm medium. Once sufficient numbers of DRGs were isolated, they were carefully placed around the inserts in a drop of medium, with three or four DRGs per well. After 3 hours at 37°C, the inserts were lifted out, and the wells were filled very slowly with medium. The following day, the medium was removed and 4% PFA in PBS was added. After 10 minutes, wells were washed

with PBS, and the DRGs were stained with phalloidin-TRITC and viewed under an Olympus fluorescence microscope or a Leica PS5 confocal microscope.

Implants

Implants were prepared from a thin film of PCL (30–40 kDa) made by drying on glass from an ethyl acetate solution. Antibody was concentrated to over 10 mg/mL and allowed to dry on the film at room temperature under laminar flow. CSIC002 in ethanol was applied and allowed to dry. The resulting dry mixtures were granulated and extruded into a 0.3-mm diameter cylinder. Sections were prepared in lengths of 2, 5, and 10 mm. The diameter was compatible with application via a 23-G needle.

Intravitreal PCL Implants

PCL implants were prepared using Nile Blue as a dye to permit observation. When applied in the rabbit vitreous, the implant remained visible for 3 months. The degradation time of the PCL implant was on the order of 6 months. The pharmacokinetics of CSIC002 was assessed in mice via intravenous (3.3 mg/kg in serum) and intravitreal (0.19 µg/eye as suspension) routes. Intravitreal application was not associated with signs of toxicity or inflammation. Intravitreal administration of Fab 3H4 in rats was likewise well tolerated.

The function of the implants was tested in a model elution system. The implant was placed in the 1-mL chamber of the system containing hyaluronic acid (stabilized with 0.1% NaN_3) to simulate the rabbit vitreous. Syringe pumps were used to slowly push 0.1% NaN_3 in saline (0.9% NaCl) through the chamber at 1 mL/day. The liquid was collected and measured daily.

In Vivo Assay for Rat Optic Nerve Transection

The axotomy model has been previously described.[22] The left optic nerve of anesthetized male Sprague-Dawley rats (8–10 weeks old, 300 g) was axotomized with minimal impairment to the meninges and leaving the optic nerve blood supply intact. The microsurgery was done using specially designed glass dissector with a 200 µm tip and a smooth blunt edge.[34] This permitted the insertion in the nerve bundle without opening of associated vessels.

Rabbit Model of Nonarteritic Ischemic Optic Nerve Neuropathy

A new method to create nonarteritic ischemic optic nerve neuropathy (NAION) in rabbits was developed for these studies. Healon solution (Abbott, 10 mg/mL of 3% sodium hyaluronate) was used as a slow release vehicle due to its viscosity, sterility, and intravitreal compatibility. Endothelin-1 (ET-1; Merck, 0.1 mg vial), a vasoconstrictor peptide, was used to initiate NAION via local vasoconstriction of vascular supply to the head of the optic nerve. A total volume of 25 µL of 30% Healon solution containing 0.05 mg ET-1 and methylene blue was injected such that the bolus was placed directly on the optic disc of a rabbit. Fluorescein angiography performed 24 hours following the intraocular injection demonstrated that the blood supply emanating from the optic disc was completely occluded.

Rabbit Model of Acute Glaucoma

Acute glaucoma was induced in rabbits by introducing a maintainer cannula (used in cataract surgery) into the anterior chamber of the right eye. The maintainer was connected to an intravenous infusion set with saline. The vial of the saline was raised at a height of 1 m. The column of water in the system created an intraocular pressure of 45 to 50 mm Hg. This acute change in pressure induces total collapse of the retinal blood vessels. The pressure was maintained for 1 hour. This condition induces death of the RGCs.

Retrograde Labeling of RGCs and the Evaluation of Their Survival

As previously described,[22] small crystals of the lipophilic neurotracer dye 4-(4-(didecylamino) styryl)-*N*-methylpyridinium iodide (4-Di-10-Asp) were dissolved in mineral oil (adjuvant grade) and placed at the axotomy site in rats. Retrograde transport (via extant microtubule networks in viable axons) allows 4-Di-10-Asp to reach and label live innervated RGCs but not dead ones.[35] Four days after the application, retinas were excised, fixed, and visualized using fluorescent microscopy. The labeled RGCs were counted as previously described.[22,36]

In Vivo Drug Administration and Assay Termination

The drugs were administered to the eyes 24 hours after the insult. The rationale for this protocol is that in our previous experience Sema-3A is detected beginning 24 hours following an injury. Analyses were performed 14 days following the insults in all of the in vivo trials.

Implant Derived Inhibitors

In drug delivery, it is necessary to demonstrate that the active ingredient retains function after release from an implant. For scratch and repulsion assays with Fab 3H4 that was released from an implant, implants loaded with 0.6 mg of Fab 3H4 (9–10 mm; approximately 200 µg 3H4) and blank (no Fab 3H4) implants were incubated for 5 days in 100 µL of DMEM at 4°C prior to the experiments. For scratch and repulsion assays with CSIC002 released from an implant, 2-cm implants loaded with CSIC002 (approximately 400 µg CSIC002) and blank implants were incubated for 7 days in 100 µL of DMEM at 4°C prior to the experiments.

Statistics

The P values were determined by 1-way ANOVA using GraphPad Prism 9 software. The P values < 0.05 were considered to be statistically significant.

Results

Synthesis of CSIC002

The synthetic route for the preparation of CSIC002 is shown in Figure 1. Because of the trimer peptoid nature of this compound, the route involved the independent preparation of the three fragments followed by coupling reactions. The intermediates and CSIC002 were fully characterized by spectroscopic methods, and purities were determined by analytical HPLC. CSIC002 is derived from the previously described Sema-3A peptoid inhibitor, SICHI1.[35,36] An aromatic carbamate was introduced at the secondary amino group of SICHI1 to create CSIC002. This residue improves the physicochemical properties resulting in continuous release from the implant and slower clearance from the eye.

Isolation and Evaluation of Sema-3A-Specific Antibodies

Sema-3A-specific antibodies were isolated by antibody phage display, as described in the Methods section. A total of 16 different (at the sequence level) Sema-3A-specific phage antibodies were isolated, and corresponding IgGs were shown to be specific for Sema-3A by ELISA. Binding to three control antigens (BSA, streptavidin, and maltose-binding protein fused to LacZ [MBP-LacZ]) was negligible (Supplementary Fig. S1). The apparent binding affinities were determined (Supplementary Fig. S2). Although the affinity of antibody 3G3 for Sema-3A was higher than the affinities of the other tested antibodies, 3G3 did not inhibit Sema-3A-mediated signaling. Of the isolated antibodies, 3H4 was the best inhibitor of Sema-3A-mediated signaling. Antibodies with moderate binding affinities are usually not suitable for evaluation in vivo without further affinity maturation. However, in our experimental system, antibodies were administered into the very confined space of the eye vitreous, and such affinities can be sufficient to achieve an antibody-mediated effects.

Sema-3A Leads to Cell Contraction that is Partially Blocked by Sema-3A Antibody

U87MG cells express neuropilins and secrete Sema-3A.[37] We exposed U87MG cells to a range of Sema-3A concentrations and showed that a concentration range of 250 to 500 ng/mL optimally induced morphological changes in the cells (Supplementary Fig. S3). We then compared the effect of a known inhibitor of Sema-3A, the compound SICHI1,[38,39] and its analogue CSIC002 on morphological changes induced by Sema-3A. We observed almost no difference in the morphology of cells exposed to Sema-3A with an inhibitor and the morphology of cells exposed to Sema-3A alone. In both cases, the cells contracted dramatically in comparison to the control cells that were either not treated or that were exposed only to inhibitor. Partial rescue of Sema-3A contraction was detected in the presence of function-blocking anti-Sema-3A Fab 3H4 antibody but not with a second anti-Sema-3A antibody (clone MABN783; Millipore; Supplementary Fig. S4). We previously developed MABN783 and used it to detect Sema-3A in Western blot and immunohistochemical analyses.[24–26,40]

Sema-3A-Mediated Inhibition of Cell Migration is Rescued by Sema-3A Inhibitors

Because CSIC002 had little effect on U87MG cell morphology, we analyzed the effects of this inhibitor using the scratch assay. We first confirmed that Sema-3A hindered U87MG migration into the scratch gap, and then we tested the ability of Sema-3A inhibitors to neutralize the inhibitory effects of Sema-3A on cell migration. In the presence of CSIC002, significantly more cells were able to migrate through the scratch than when cells were incubated with Sema-3A alone (Fig. 2A). Of the 18 Sema-3A binding Fabs isolated, Fab 3H4 was the best inhibitor of Sema-3A activity. Quantification of cells in the scratch after 24 hours of exposure showed that in the presence of Fab 3H4 the number of cells that entered the gap was significantly

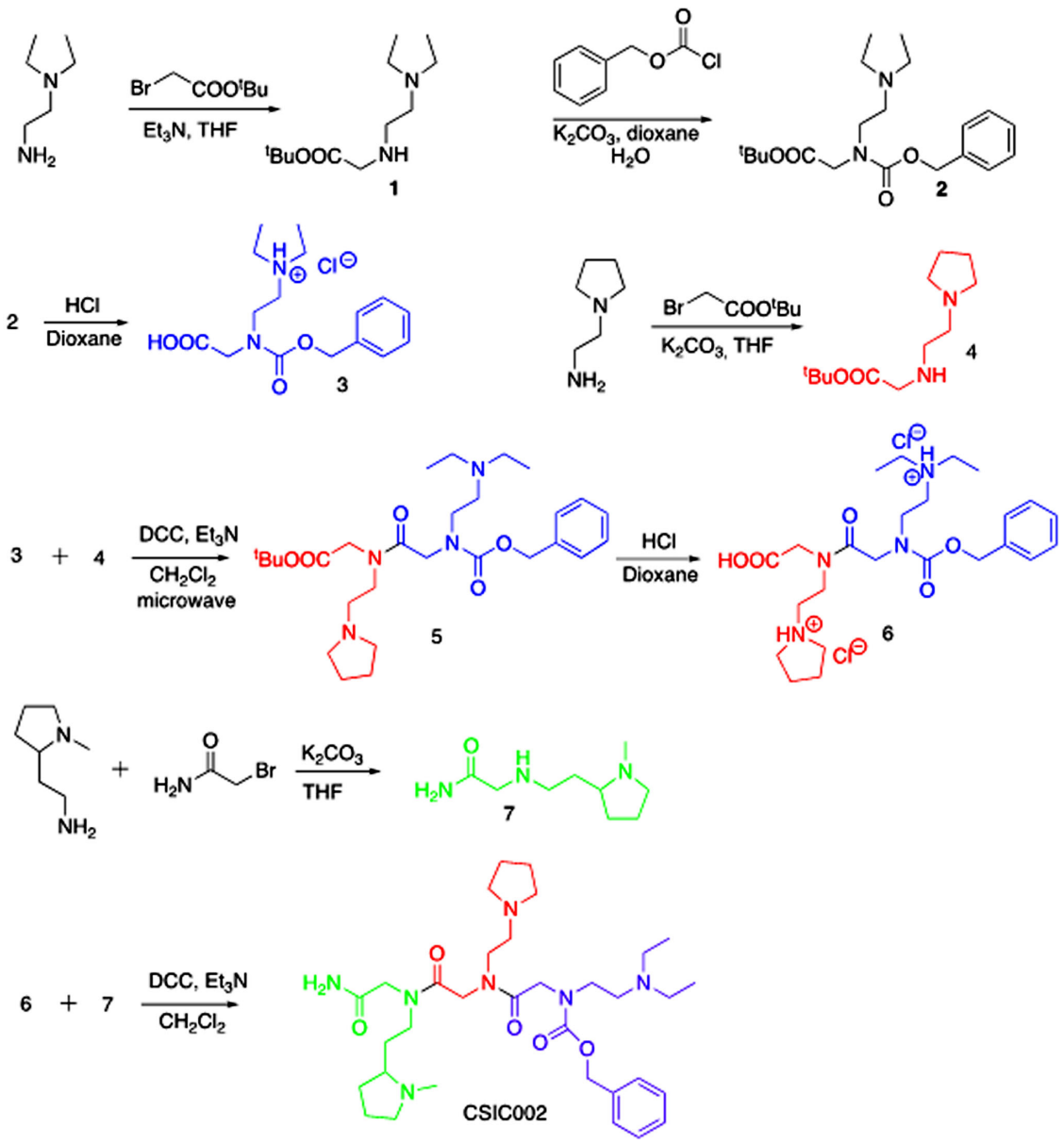

Figure 1. **Scheme for the preparation of CSIC002.** The fragments of the trimer are color coded.

higher than when cells were exposed to Sema-3A alone (Fig. 2B). Cells exposed to the inhibitors alone displayed behavior similar to that of the untreated cells (Supplementary Fig. S5). In summary, we observed that U87MG cells exposed to Sema-3A were slower in closing the gap than cells not exposed to Sema-3A and that Sema-3A inhibitors mitigated the effects of Sema-3A.

Controlled Release of Sema-3A Antagonists Inhibits Deleterious Effects of Sema-3A

Biodegradable implants are one means of prolonged and controlled drug release. Given the role of Sema-3A in chronic diseases, we tested the efficacy of these antagonists following their incorporation into and release from such implants. For that purpose, we constructed two types of biodegradable implants: the first made from a combination of poly-lactic acid (PLA) and poly-lactic-glycolic acid (PLGA) and the second made from PCL. The PLA/PLGA implants are suitable for formulation of low-molecular weight and stable molecules but due to the organic solvents and high temperature needed for their production they are detrimental for proteins. To overcome this limitation, we fabricated implants from PCL, which is a biologically degradable linear polyester. PCL has a low melting point

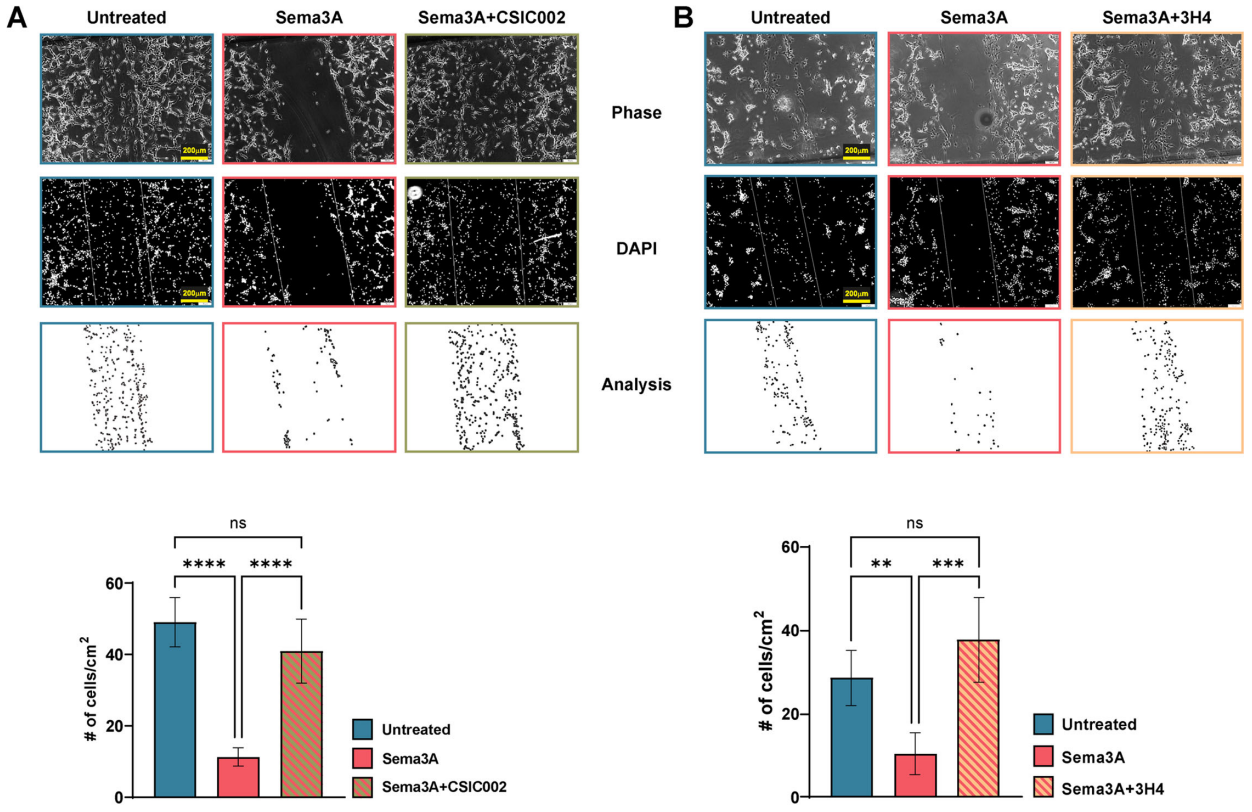

Figure 2. CSIC002 and Fab 3H4 rescue Sema-3A-mediated inhibition of cell migration. (**A**, **B**) Upper: Representative images of U87MG cells seeded at 3×10^4 per well, scratched after 2 days, treated or not, and imaged after 24 hours. Cells were treated with vehicle, with Sema-3A (250 ng/mL), or with Sema-3A pre-incubated with **A** 10 µM CSIC002 (bars = 200 µm) or **B** 10 µg/mL of Fab 3H4. Shown are top to bottom, phase contrast, DAPI signal (bars = 200 µm). Lower: The number of cells per cm^2 in the scratch quantified using ImageJ software. $^{**}P < 0.01$, $^{***}P < 0.001$, $^{****}P < 0.0001$. Each experiment was performed in triplicate and repeated three times. ns, nonsignificant.

(60°C), which permits extrusion without subjecting the active substances to potentially denaturing conditions.

The kinetics of release for both classes of compounds were measured using a laboratory system, created for the presented study that mimics aqueous flow through the vitreous humour in the eye. PCL implants loaded with 30% wt/wt CSIC002 released 80% of the total active substance in 15 days. An implant of 1-cm length containing approximately 200 µg of CSIC002 released at least 11 µg/day over the first 9 days, followed by a slower release for the next 6 days. There was a maximum peak of 52 µg/day on day 3. Fab 3H4 loaded in the implant at 33% wt/wt antibody had elution kinetics that were similar to those of CSIC002 (Supplementary Fig. S6).

Loaded implants were then incubated for 7 days in Dulbecco's modified Eagle's medium (DMEM) and the obtained solutions, containing the released compounds were tested in scratch assays. Solutions of DMEM incubated with empty implants for 7 days had no effect on cell migration with or without Sema-3A (Fig. 3A). Following release from the implant, CSIC002 significantly blocked the destructive effects of Sema-3A on cell migration as effectively as a standard CSIC002 solution (Fig. 3B). Similarly, the anti-Sema-3A Fab 3H4 released from PCL was as effective as unformulated antibody and significantly restored cell migration (Fig. 3C). Interestingly, the mere presence of the inhibitory compounds even without addition of Sema-3A improved cell migration into the scratch compared with untreated cells.

Sema-3A Inhibitors Rescue Axonal and Growth Cone Collapse Resulting from Sema-3A Treatment

To further validate the inhibitory capabilities of CSIC002 and Fab 3H4, we developed a repulsion assay, which was carried out using a coculture of HEK293 cells, which secrete Sema-3A, and chicken embryo

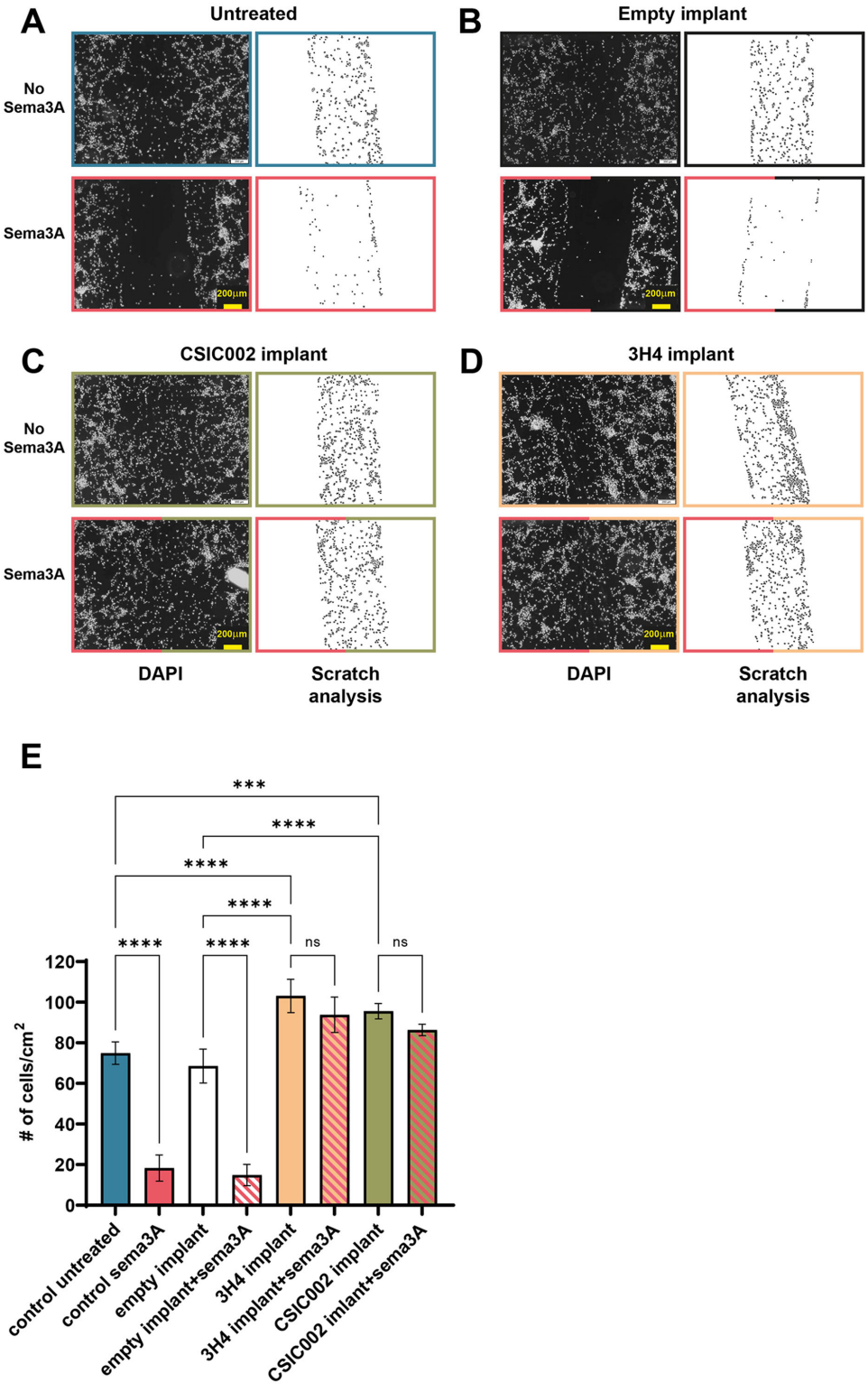

Figure 3. Controlled release of Sema-3A inhibitors from 100% PCL implants rescue deleterious effects of Sema-3A on cell migration. (**A–D**) Representative images of scratch assays performed with U87MG cells. **A** Left: The controls were incubated with DMEM (untreated) or with Sema-3A. **B** The "empty implant" cells were treated with a solution that had been incubated with an unloaded 100% PCL implant either with or without Sema-3A. **C** Cells were incubated with DMEM containing 20 µM of CSIC002 released from an implant with or without Sema-3A. **D** Cells were incubated with DMEM containing 10 µg/mL of Fab 3H4 released from an implant with or without Sema-3A. (**E**) Quantification of the effects of CSIC002 and Fab 3H4 secreted from PCL implants on Sema-3A chemo-repellent activity (bars = 200 µm). ***$P < 0.001$, ****$P < 0.0001$. ns, nonsignificant.

DRGs (Fig. 4A). The Sema-3A-secreting HEK293 cells were seeded inside an ibidi insert in PDL-coated wells. On the day of the experiment, the wells were coated with laminin around the ibidi insert, but not inside it, and the DRGs were placed around the insert. DRGs were allowed to attach to the surface of the well. The insert was then removed allowing both types of cells to share the same medium. Because Sema-3A elicits growth cone collapse,[5,7,41] the DRGs, for the most part, did not extend axons toward the HEK293 cells, and the few axons that did grow had a collapsed phenotype (Fig. 4B).

We used this assay to analyze the effects of Sema-3A inhibitory molecules on axon extension and growth cone collapse. Axons and growth cones were detected with phalloidin and visualized utilizing fluorescent microscopy. Almost no axonal extension was observed in DRGs at the side facing the HEK293 Sema-3A expressing cells (Fig. 5). In contrast, in DRGs treated with Fab 3H4 antibody, axonal growth and associated growth cone sprouting were detected (see Fig. 5). In the presence of CSIC002, less axonal growth was detected in cultures treated than in the presence of Fab 3H4, but the axons that did grow had very long processes (see Fig. 5). Solutions from inhibitor-loaded PCL implants were also highly effective in neutralization of the effects of Sema-3A on axonal growth and sprouting (Fig. 6). Mean intensity of phalloidin fluorescence was measured in increments of 50 µm from the DRG core toward the Sema-3A-secreting HEK293 cells. The mean intensities of the DRGs were almost the same 50 µm away from the core for all treatments, but intensities dropped dramatically the further the measurement is taken. Typically, at 550 to 650 µm distance from the core, the intensity measured was due to sprouting axons with no cell bodies. Within that area, the intensity of the phalloidin was more than 2.5-fold higher in the samples treated with Sema-3A inhibitors than in samples treated with the blank implants (Supplementary Fig. S7).

Clearance of Fluorescently Labeled Anti-Sema-3A Antibodies from Rat Eyes Altered by Axotomy

Using the Maestro imaging system, we measured the kinetics of clearance of fluorescently labeled Fabs that bind to Sema-3A from rat eyes subjected or not to optic nerve axotomy. Our previous results showed that levels of Sema-3A are increased in the retina following axotomy.[22] We injected fluorescently labeled Fab 3H4 into the vitreous of eyes of axotomized rats and control rats and measured fluorescence in the eye over time (Fig. 7A). The greatest disparity between the groups was detected 24 hours after injection. In the control group, not subjected to axotomy, Fab 3H4 was mostly cleared during the first 24 hours, declining by more than 80% from the initial signal. In the axotomized group, however, the decline of the signal was slower

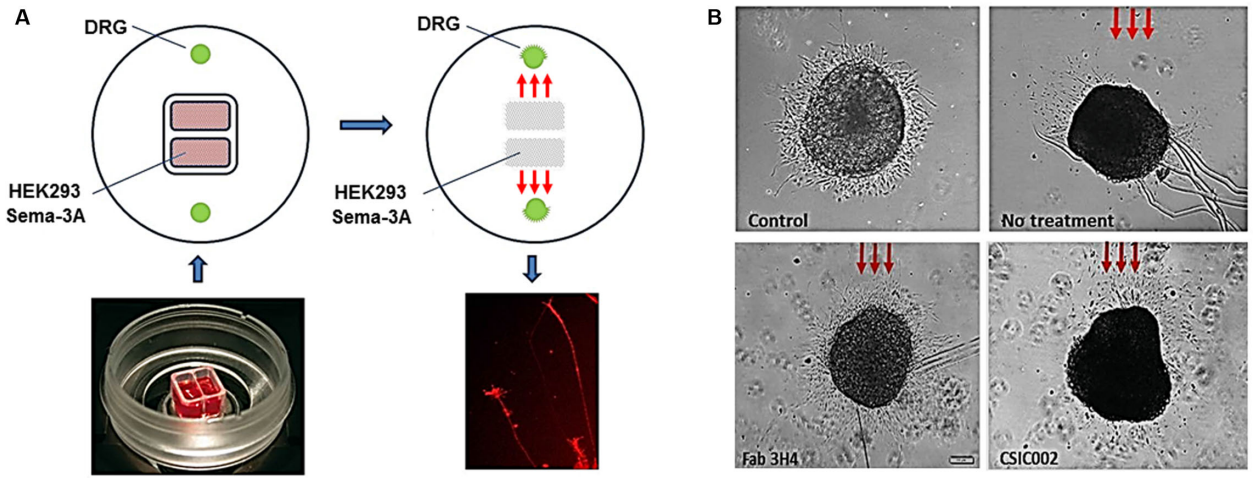

Figure 4. **DRG repulsion assay**. (**A**) For the repulsion assay, ibidi inserts were placed in the middle of each well in a 12-well plate that was coated with PDL. Inside the insert, we seeded 3 × 10^5 HEK293-Sema-3A secreting cells and incubated overnight at 37°C. The wells were coated with laminin around the ibidi insert, but not inside it. After 2 hours, DRGs were positioned individually around each insert and were incubated for 3 hours in a drop of medium to encourage attachment to the surface. The inserts were then removed, and the wells were filled with medium with or without Sema-3A inhibitors and incubated for another 24 hours at 37°C. The red arrows point at the direction of Sema-3A flow. (**B**) Representative bright-field images of DRGs growth in the absence of Sema-3A-secreting HEK293 cells (control) or in the presence of HEK293 cells, without inhibitor (no treatment), with 10 µg/mL of Fab 3H4 or with 10 µM of CSIC002. Red arrows indicate the position of the HEK293-Sema-3A cells in respect to the DRGs.

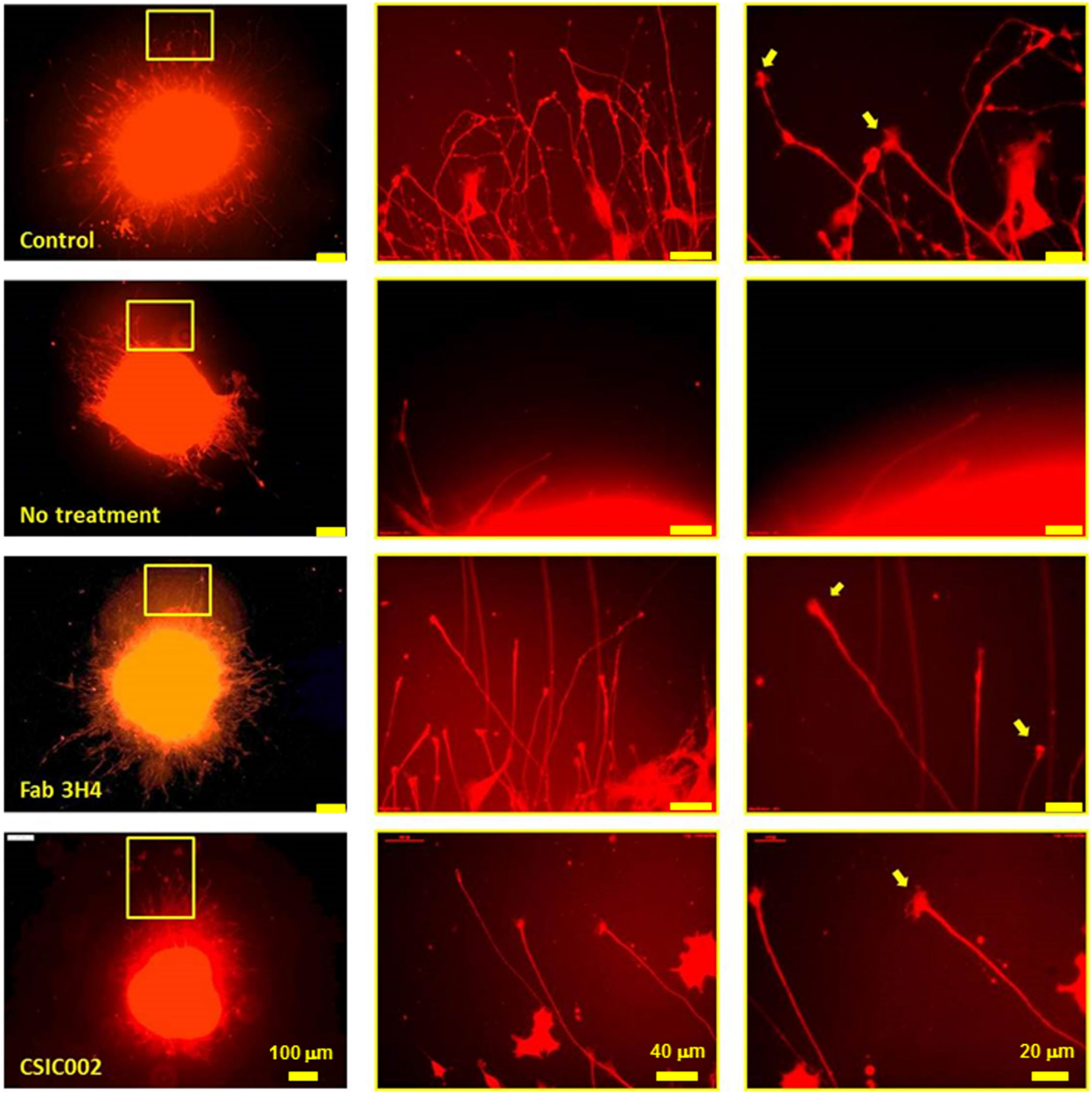

Figure 5. **Fab 3H4 and CSIC002 mitigate the effect of Sema-3A on DRGs.** The DRG repulsion assay was performed in the absence of HEK293 cells (control), in the presence of Sema-3A-secreting HEK293 cells (no treatment), and in the presence of HEK293 cells in medium containing Fab 3H4 (10 µg/mL) or CSIC002 (10 µM). DRGs were fixed and stained with phalloidin to reveal actin stress fibers. The columns to the left show representative DRGs at low magnification (bar = 100 µm). Yellow rectangles indicate the region of the DRGs magnified in the middle column (bar = 40 µm). Columns to the right show higher magnification images with intact growth cones indicated by yellow arrows (bar = 20 µm).

with around 50% lost in the first day (Fig. 7B). After 48 hours, both signals were low, but the fluorescence emanating from the eyes of the axotomized group were 2-fold higher than the signal from the control group (see Fig. 7B). Although axotomy significantly slowed the clearance of 3H4 Fab, no such effect was detected for a non-specific anti-streptavidin antibody (Fig. 7C). These data suggest that the higher levels of Sema-3A that result from axotomy are responsible for slower clearance kinetics of Fab 3H4.

Sema-3A Inhibitors Protect RGCs Following Axotomy, Glaucoma, and NAION

To examine whether the function-blocking antibody raised against Sema-3A and the low-molecular weight

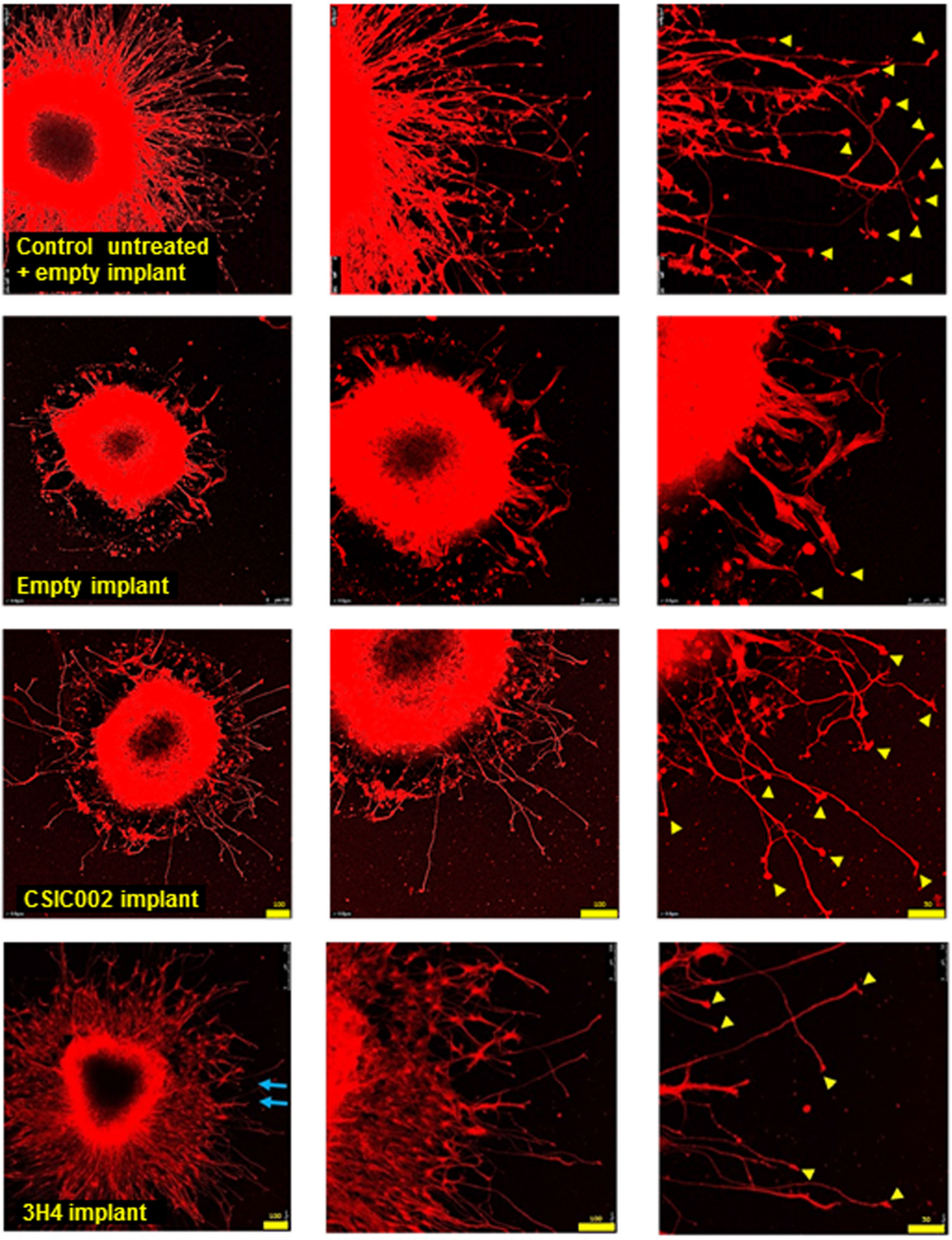

Figure 6. **Axon sprouting and intact growth cones detected in DRGs treated with inhibitors secreted from PCL implants.** The repulsion assay was performed in the absence of HEK293 cells (control untreated), in the presence of Sema-3A-secreting HEK293 cells (no treatment), and in the presence of HEK293 cells in medium containing Fab 3H4 (10 µg/mL) or CSIC002 (20 µM) secreted from PCL implants. DRGs were fixed and stained with phalloidin. The columns to the right show low magnification images (bars = 100 µm). The middle and left columns show higher magnification images (bars = 100 µm and 50 µm, respectively). Yellow arrows indicate intact growth cones.

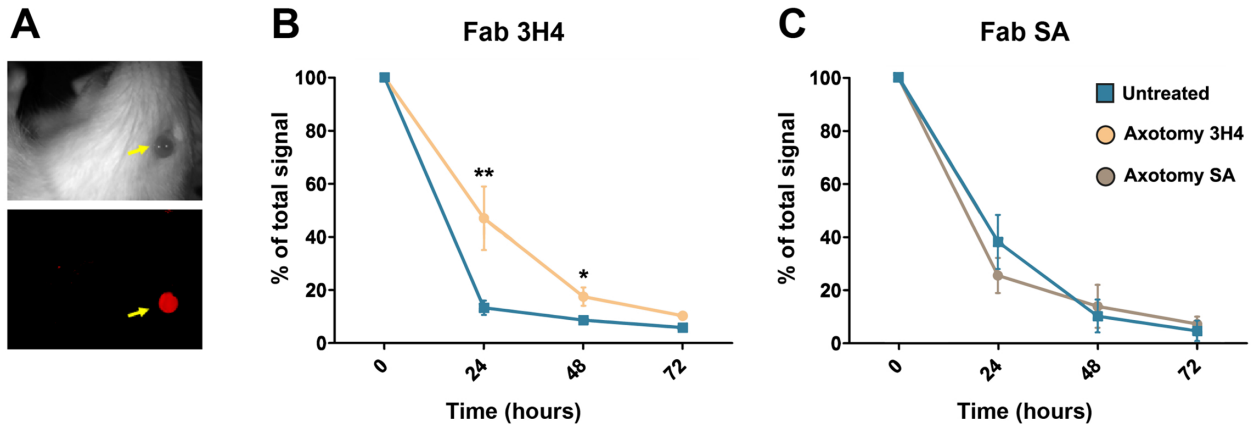

Figure 7. Clearance rate of anti-Sema-3A Fabs from rat eyes is altered by axotomy. The 1.5 mg/mL anti-Sema-3A and nonspecific antibodies were fluorescently labeled. After labeling and purification (removal of the free dye), the final concentration was 0.6 µg/mL, 3 to 4 µL were injected into rat eyes. (**A**) Photograph (top) and fluorescent image (bottom) of the eye of a rat (yellow arrow) immediately after intravitreal injection of Fab 3H4 conjugated with Alexa fluor 680 dye. (**B**) Quantification of the fluorescence emanating from the eyes of rats either subjected to axotomy (orange) or not (blue) and injected with 3H4 Fab conjugated with Alexa fluor 680 into the vitreous. The fluorescence was quantified every 24 hours for 3 days ($n = 3$). (**C**) Quantification of the fluorescence due to fluorescently labeled anti-streptavidin Fab (Fab SA; $n = 3$) from eyes of rats subjected to axotomy (grey) or not (blue) treated intravitreally with Fab SA. Plotted are means ± SD. *$P < 0.05$, **$P < 0.005$.

CSIC002 attenuate axotomy-induced RGC degeneration in a rat model, the inhibitory molecules were injected intravitreally into the axotomized eyes 24 hours after surgery, and RGC viability was monitored 14 days later. The intravitreal injection consisted of 3 to 4 µL of Fab 3H4 (1 mg/mL) in PBS or CSIC002 (10 µM) in PBS. Untreated eyes were injected with 3 to 4 µL of PBS. In untreated rats, less than 5% of

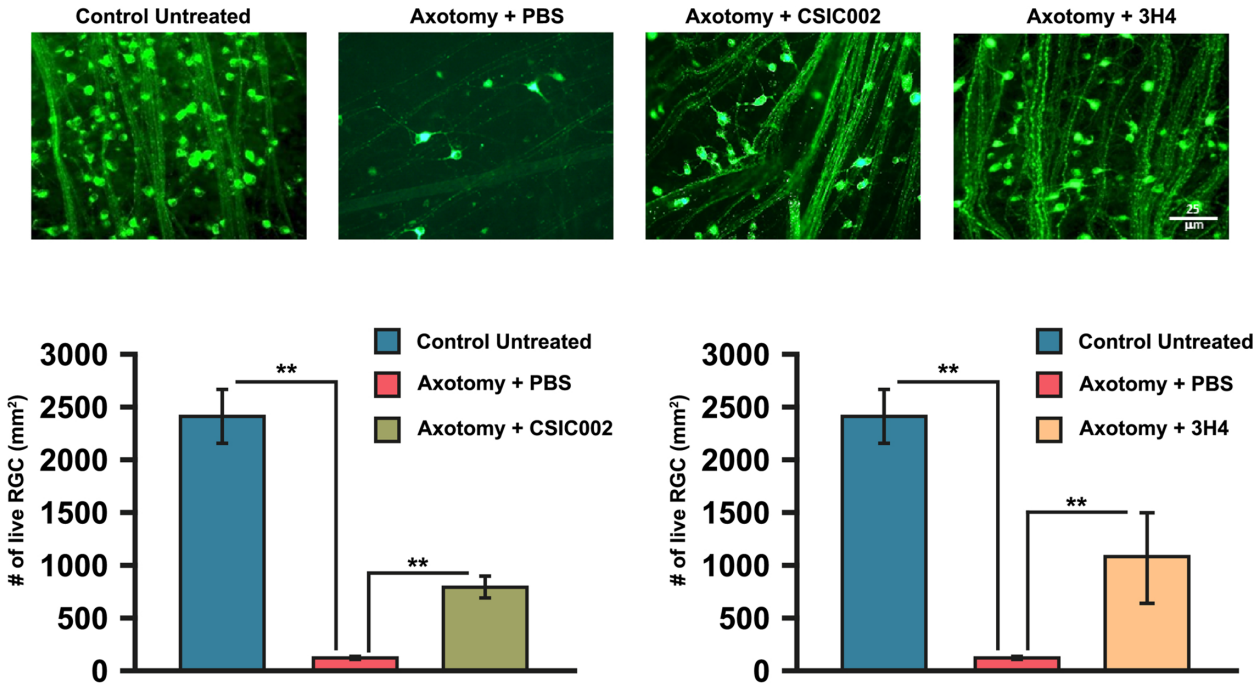

Figure 8. Sema-3A inhibitors protect RGCs following axotomy of the optic nerve in rats. Upper: Representative images of retrograde labeling of live RGCs from retinas of rats not subjected to axotomy (control, untreated), rats subjected to axotomy and mock treated (axotomy + PBS), and rats subjected to axotomy treated with intravitreal injection of CSIC002 (10 µM) or Fab 3H4 (1 mg/mL). Injections were administered 24 hours after injury, and RGC labeling was performed 14 days later. Lower: Plots of the numbers of live RGCs from each treatment ($n = 3$ for each group, 8–15 different images were counted from each retina). **$P < 0.005$.

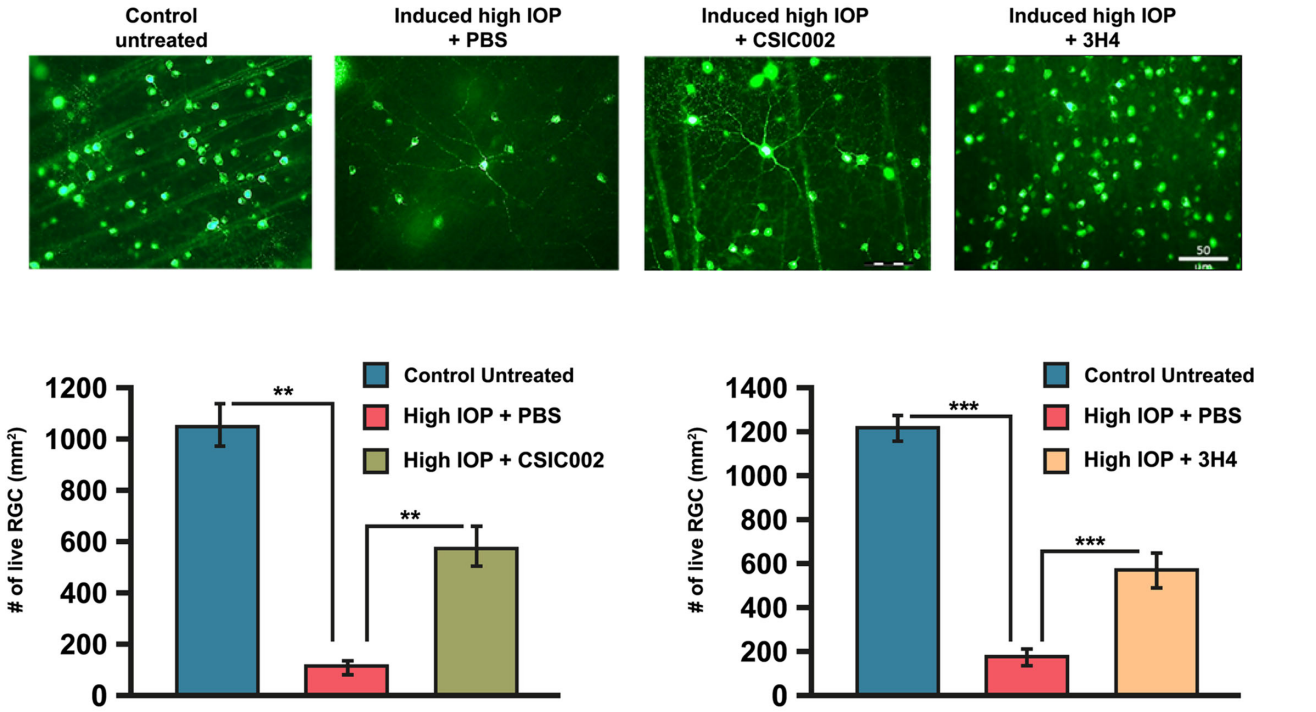

Figure 9. Sema-3A inhibitors enhance RGC survival in a rabbit acute glaucoma model. Upper: Representative images of retrograde labeling of retinas in control rabbits and rabbits subjected to high intraocular pressure that were mock treated (+ PBS) or that were treated with CSIC002- or Fab 3H4-loaded implants. Implants were inserted 24 hours after glaucoma induction, and RGC labeling was performed 14 days later. Lower: Plots of the numbers of live RGCs from each treatment ($n = 4$ for each group, 8–15 different images were counted from each retina). $^{**}P < 0.005$, $^{***}P < 0.0005$.

RGCs survived after axotomy. Intravitreal injection of CSIC002 or of Fab 3H4 led to the survival of around 33% and 45% of the axotomized RGCs, respectively (Fig. 8).

Significant protection of RGCs was also detected in acute glaucomatic rabbits following treatment with implants containing CSIC002 or Fab 3H4. CSIC002 was dosed from a 2-cm long, 0.3-mm diameter of 100% PCL implant containing 7 µg/mL CISC002. For Fab 3H4, the 100% PCL implants were 3 cm long and 0.3 mm in diameter that contained 10 µg/mL Fab 3H4. In this model, 55% RGC survival was observed in CSIC002-treated eyes and 46% survival was observed in Fab 3H4-treated eyes compared to about 10% in untreated eyes (Fig. 9). Delivery of 7 µg/mL CISC002 using a 100% PCL implant also protected RGCs following NAION induction. Implants loaded with CISC002 led to 48% RGC survival compared to only 8.1% survival in untreated eyes (Fig. 10). Similar to the axotomy model, implants were inserted into the eyes of rabbits 24 hours following acute glaucoma or NAION induction, and RGC survival was assessed 14 days after the surgery.

Discussion

Sema-3A is involved in response to injury and stress, and high levels are associated with loss of neuronal tissue. Sema-3A is upregulated after acute injury, such as optic nerve axotomy[40] and in a rat model of retinal detachment.[24] Sema-3A is chronically induced in degenerative diseases, such as glaucoma[24] and in the genomic instability disorder Nijmegen breakage syndrome.[26] We previously directly demonstrated the destructive role of Sema-3A in the prevention of neural regeneration.[25] Thus, specific neutralization of Sema-3A action should be beneficial in treating various brain and retinal degenerative diseases.

Here, with the goal of neutralizing the deleterious effects of Sema-3A, we tested two types of Sema-3A inhibitors. The first was the low-molecular-weight inhibitor CSIC002. Only two small-molecule inhibitors of the Sema-3A pathway have been generated thus far: xanthofulvin and SICHI1. Kaneko et al. identified xanthoflavin as a strong and selective inhibitor of Sema-3A signaling by screening of fermentation

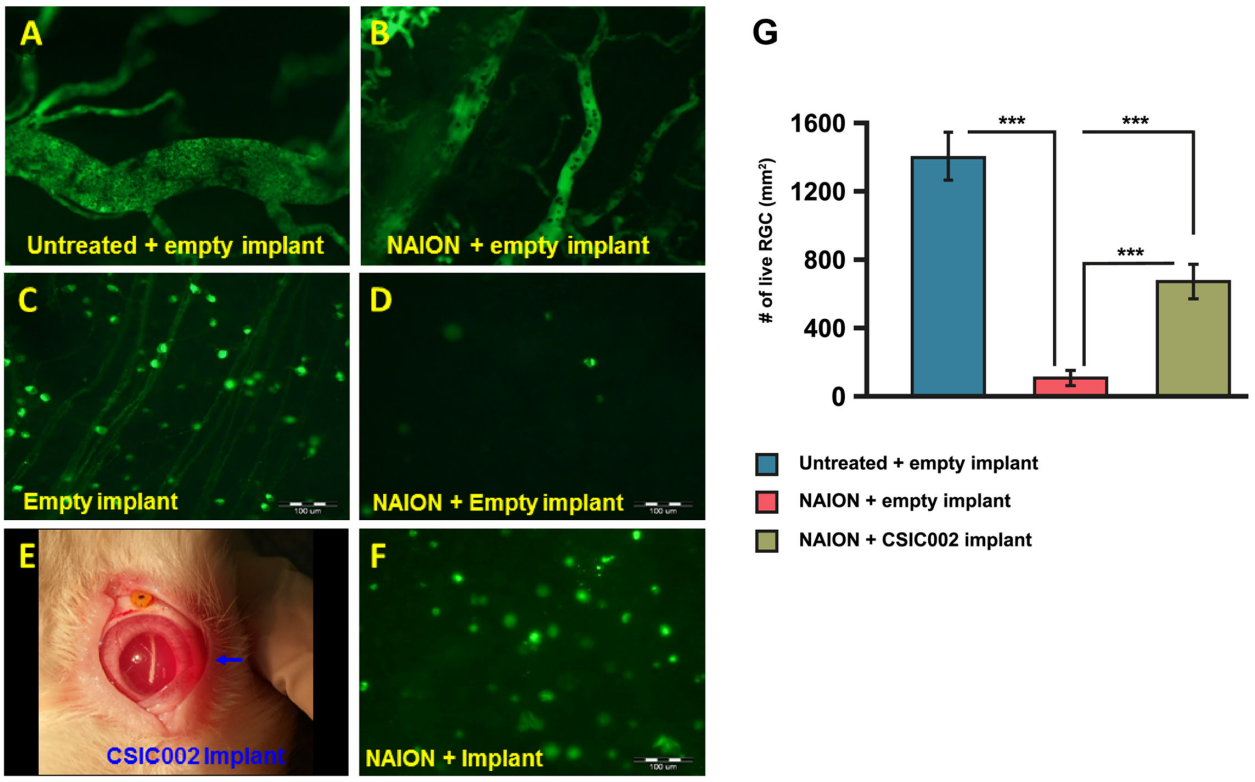

Figure 10. Sema-3A inhibitors protect RGCs following NAION in rabbits. Fluorescein angiography of control untreated (**A**) and NAION subjected retinas (**B**) implanted with empty implants. Representative images of retrograde labeling of retinas not subjected to NAION control (**C**) or NAION subjected (**D**) injected with an empty implant. (**E**) A picture of rabbit eye injected with 100% PCL implant 24 hours after NAION induction. (**F**) Representative images of retrograde labeling of retinas subjected to NAION implanted with a CSIC002-loaded implant following NAION in rabbits. (**G**) Plot for the number of live RGCs from each treatment ($n = 5$ for each group). Implants were inserted 24 hours after NAION induction. Fluorescein angiography and RGC labeling were performed 14 days following surgery. ***$P < 0.0001$.

broth of a fungal strain.[42] Even though xanthofulvin enhances nerve regeneration in axotomized axons in the olfactory system, its direct interaction with Sema-3A has not been shown. SICHI1 was identified from a peptoid combinatorial library.[35,36] The analog CSIC002 has an aromatic carbamate at the secondary amino group that enhanced pharmacodynamics relative to SICHI1.

Antibodies have also been shown to be potent Sema-3A inhibitors. We demonstrated previously that a polyclonal function-blocking anti-Sema-3A antibody capable of neutralizing Sema-3A activity rescued sympathetic neurons from dopamine-induced toxicity.[21] Furthermore, intravitreal injection of this antibody rescued over 80% of the RGCs in rabbit axotomized eyes for more than 2 weeks.[22] Although polyclonal antibodies can serve as valuable scientific research tools, they are not suitable as drugs. Therefore, we screened a human antibody phage display library and identified a function-blocking Fab, Fab 3H4.

Three different assays were used to analyze the efficacies of these agents as function-blocking inhibitors in vitro: Sema-3A-induced U87MG cell contraction, Sema-3A-induced U87MG cell migration, and chick DRG axonal repulsion. The quantitative chemorepulsion assay described by He and Tessier-Lavigne[43] is a multistage procedure that takes several days to perform and requires a great deal of experience. We developed a semiquantitative repulsion assay using chick embryo DRGs that is markedly less time consuming and that provides reliable assessment of the efficacy of Sema-3A inhibitors. The chemorepulsive activity of Sema-3A[44] as well as its effects on cell contraction[45] are mediated by neuropilin1 and plexin A1, whereas cell migration is modulated via neuropilin 2 and plexin A1.[46] That all these activities were neutralized by CSIC002 and Fab 3H4 suggest these inhibitors act directly on Sema-3A rather than on factors that mediate Sema-3A activity.

Various kinds of biodegradable implants are currently used to enable controlled release of different drugs. Here, we showed that the inhibitory effects of the low-molecular-weight CSIC002 and the function-blocking Fab 3H4 were not negatively affected by

loading them into implants. Moreover, in the scratch assay, compounds released from implants enhanced cell migration without the addition of Sema-3A, and in the repulsion assay more axons with active growth cones appeared to have sprouted from the DRGs treated with the implant-released compounds than the DRGs treated with compounds directly, although this was not quantified due to the limitations of the assay. The reasons for these intriguing results are not known. U87MG cells secrete Sema-3A[37] and that may explain the beneficial effect of implant-released compounds on cell migration, even in the absence of added Sema-3A. The implant itself and the materials associated with it were not beneficial to cell migration because results from assays with untreated controls and unloaded implants were similar. Because the intra-implant concentrations of the Sema-3A inhibitors is similar to the direct injection, it led us to speculate that the loading into and release from the implants removed certain materials that have nonspecific inhibitory effects on cell migration and axonal growth. Alternatively, it is possible loading and release altered the three-dimensional structures of the inhibitors.

The efficacies of Sema-3A inhibitors CSIC002 and Fab 3H4 and the validities of the in vitro tests described here were substantiated using in vivo tests in which the inhibitors rescued RGCs following optic nerve axotomy and acute glaucoma. These data suggest that timely application of Sema-3A antagonists considerably increases RGC survival in the lesioned eye. Due to the complexity of these models, it was not possible to conduct dose response analyses, and thus it remains unclear whether the approximately 50% survival observed could be increased with a higher dose of inhibitor or whether pathways not mediated by Sema-3A also cause RGC loss. In addition to issues of dose, residence time in the eye is also a critical factor. The vitreous is subject to dorso-ventral aqueous flow that efficiently removes substances from the retinal surface. The half-lives of optimized Fabs in the eye is in the range of 16–24 hours. In anticipation of such effects, we tested the use of a PCL implant that permits very high loading of active ingredients. CSIC002 and Fab 3H4 formulated in implants effectively prevented Sema-3A-mediated RGC loss in models of acute glaucoma and NAION induction, respectively.

Models of this type are by necessity acute and relatively extreme in terms of pathology. In axotomy, RGC loss is persistent. In ocular hypertension and endothelin-mediated vasoconstriction, it is transient. In the models used, we applied the antagonists immediately after injury. The observation that RGCs are protected from both acute and persistent stress by Sema-3A inhibitors suggests that these compounds may have clinical utility. In settings such as glaucoma not associated with increased intraocular pressure, regular treatment with a Sema-3A inhibitor may be sufficient to protect RGCs even if the causes of their loss persist. In the context of trauma to the eye where there is a transient stress, the application of such antagonists may allow the RGCs to survive the initial stress reaction and thus retain function once injury-related remodeling is complete. Whether this is the case or not will require longer term observations. It will be especially important to determine whether antagonism of Sema-3A leads to a permanent loss of this signaling cascade or whether signaling accumulates or breaks through once the antagonist is depleted from the site of application. There is a rationale for creating both low molecular weight anti-Sema-3A inhibitors and Sema-3A neutralizing antibodies. In many acute or chronic neurodegenerative conditions, the immune system is dysfunctional. In these cases, antibody treatments are not efficacious and small-molecular Sema-3A inhibitors will be necessary.

Loss of neurons in or near sites of injury remains a key problem of modern medicine. In many contexts, minor injury leads to cascades of cell loss radiating from the lesion in a manner disproportionate to the magnitude of the actual lesion. For example, strokes have a penumbra, and glaucoma proceeds at a slow rate even if pressure control is maintained. This may be related to immune privilege in the CNS and the formation of fibroblast barriers around lesions, which is a general response that is more beneficial in the context of infectious disease than in the mild lesions due to aging or injury. This "scorched earth" approach to CNS injury may be countered by neutralization of Sema-3A and perhaps a limited number of other factors to allow wound healing without inordinate sacrifice of bystander tissue, as is apparent in other organs of the body where antimicrobial innate reactions are more selective and function is usually restored following injury.

Conclusions

In summary, our findings suggest that inhibition of Sema-3A can serve as an important tool for therapeutic regimens in various CNS degenerative diseases including those of the retina, such as acute glaucoma, NAION, and injury of the optic nerve.

Acknowledgments

Funded by the EU seventh framework program, Grant Agreement #604884.

Disclosure: **A. Nitzan**, None; **M. Corredor-Sanchez**, None; **R. Galron**, None; **L. Nahary**, None; **M. Safrin**, None; **M. Bruzel**, None; **A. Moure**, None; **R. Bonet**, None; **Y. Pérez**, None; **J. Bujons**, None; **E. Vallejo-Yague**, None; **H. Sacks**, None; **M. Burnet**, None; **I. Alfonso**, None; **A. Messeguer**, None; **I. Benhar**, None; **A. Barzilai**, None; **A.S. Solomon**, None

* AB and AS contributed equally to this work.

References

1. Nakazawa T, Tomita H, Yamaguchi K, et al. Neuroprotective effect of nipradilol on axotomized rat retinal ganglion cells. *Curr Eye Res.* 2002;24:114–122.
2. Kolodkin AL, Matthes DJ, O'Connor TP, et al. Fasciclin IV: sequence, expression, and function during growth cone guidance in the grasshopper embryo. *Neuron.* 1992;9:831–845.
3. Lee WS, Lee WH, Bae YC, et al. Axon Guidance Molecules Guiding Neuroinflammation. *Exp Neurobiol.* 2019;28:311–319.
4. Hayashi M, Nakashima T. [Semaphorin and osteoporosis.]. *Clin Calcium.* 2016;26:1419–1427.
5. Luo Y, Raible D, Raper JA. Collapsin: a protein in brain that induces the collapse and paralysis of neuronal growth cones. *Cell.* 1993;75:217–227.
6. Koppel AM, Feiner L, Kobayashi H, et al. A 70 amino acid region within the semaphorin domain activates specific cellular response of semaphorin family members. *Neuron.* 1997;19:531–537.
7. Taniguchi M, Yuasa S, Fujisawa H, et al. Disruption of semaphorin III/D gene causes severe abnormality in peripheral nerve projection. *Neuron.* 1997;19:519–530.
8. Huettl RE, Huber AB. Cranial nerve fasciculation and Schwann cell migration are impaired after loss of Npn-1. *Dev Biol.* 2011;359:230–241.
9. Pasterkamp RJ, Ruitenberg MJ, Verhaagen J. Semaphorins and their receptors in olfactory axon guidance. *Cell Mol Biol (Noisy-le-grand).* 1999;45:763–779.
10. Dent EW, Barnes AM, Tang F, et al. Netrin-1 and semaphorin 3A promote or inhibit cortical axon branching, respectively, by reorganization of the cytoskeleton. *J Neurosci.* 2004;24:3002–3012.
11. Chedotal A, Del Rio JA, Ruiz M, et al. Semaphorins III and IV repel hippocampal axons via two distinct receptors. *Development.* 1998;125:4313–4323.
12. Rabacchi SA, Solowska JM, Kruk B, et al. Collapsin-1/semaphorin-III/D is regulated developmentally in Purkinje cells and collapses pontocerebellar mossy fiber neuronal growth cones. *J Neurosci.* 1999;19:4437–4448.
13. Luo Y, Shepherd I, Li J, et al. A family of molecules related to collapsin in the embryonic chick nervous system. *Neuron.* 1995;14:1131–1140.
14. Goodman CS. Mechanisms and molecules that control growth cone guidance. *Annu Rev Neurosci.* 1996;19:341–377.
15. Kolodkin AL. Growth cones and the cues that repel them. *Trends Neurosci.* 1996;19:507–513.
16. De Winter F, Holtmaat AJ, Verhaagen J. Neuropilin and class 3 semaphorins in nervous system regeneration. *Adv Exp Med Biol.* 2002;515:115–139.
17. De Winter F, Oudega M, Lankhorst AJ, et al. Injury-induced class 3 semaphorin expression in the rat spinal cord. *Exp Neurol.* 2002;175:61–75.
18. de Winter F, Cui Q, Symons N, et al. Expression of class-3 semaphorins and their receptors in the neonatal and adult rat retina. *Invest Ophthalmol Vis Sci.* 2004;45:4554–4562.
19. Spencer T, Domeniconi M, Cao Z, et al. New roles for old proteins in adult CNS axonal regeneration. *Curr Opin Neurobiol.* 2003;13:133–139.
20. Rodger J, Goto H, Cui Q, et al. cAMP regulates axon outgrowth and guidance during optic nerve regeneration in goldfish. *Mol Cell Neurosci.* 2005;30:452–464.
21. Shirvan A, Ziv I, Fleminger G, et al. Semaphorins as mediators of neuronal apoptosis. *J Neurochem.* 1999;73:961–971.
22. Shirvan A, Kimron M, Holdengreber V, et al. Anti-semaphorin 3A antibodies rescue retinal ganglion cells from cell death following optic nerve axotomy. *J Biol Chem.* 2002;277:49799–49807.
23. Solomon AS, Kimron M, Holdengreber V, et al. Up-regulation of semaphorin expression in retina of glaucomatous rabbits. *Graefes Arch Clin Exp Ophthalmol.* 2003;241:673–681.
24. Klebanov O, Nitzan A, Raz D, et al. Upregulation of Semaphorin 3A and the associated biochemical and cellular events in a rat model of retinal detachment. *Graefes Arch Clin Exp Ophthalmol.* 2009;247:73–86.
25. Rosenzweig S, Raz-Prag D, Nitzan A, et al. Sema-3A indirectly disrupts the regeneration process of goldfish optic nerve after controlled injury. *Graefes Arch Clin Exp Ophthalmol.* 2010;248:1423–1435.
26. Baranes K, Raz-Prag D, Nitzan A, et al. Conditional inactivation of the NBS1 gene in the mouse

central nervous system leads to neurodegeneration and disorganization of the visual system. *Exp Neurol.* 2009;218:24–32.
27. Meyer LA, Fritz J, Pierdant-Mancera M, et al. Current drug design to target the Semaphorin/Neuropilin/Plexin complexes. *Cell Adh Migr.* 2016;10:700–708.
28. Azriel-Rosenfeld R, Valensi M, Benhar I. A human synthetic combinatorial library of arrayable single-chain antibodies based on shuffling in vivo formed CDRs into general framework regions. *J Mol Biol.* 2004;335:177–192.
29. Good PF, Alapat D, Hsu A, et al. A role for semaphorin 3A signaling in the degeneration of hippocampal neurons during Alzheimer's disease. *J Neurochem.* 2004;91:716–736.
30. Guttmann-Raviv N, Shraga-Heled N, Varshavsky A, et al. Semaphorin-3A and semaphorin-3F work together to repel endothelial cells and to inhibit their survival by induction of apoptosis. *J Biol Chem.* 2007;282:26294–26305.
31. Bitton A, Nahary L, Benhar I. Antibody Isolation From a Human Synthetic Combinatorial and Other Libraries of Single-Chain Antibodies. *Methods Mol Biol.* 2018;1701:349–363.
32. Hakim R, Benhar I. "Inclonals": IgGs and IgG-enzyme fusion proteins produced in an E. coli expression-refolding system. *MAbs.* 2009;1:281–287.
33. Luria Y, Raichlin D, Benhar I. Fluorescent IgG fusion proteins made in E. coli. *MAbs.* 2012;4:373–384.
34. Solomon AS, Lavie V, Hauben U, et al. Complete transection of rat optic nerve while sparing the meninges and the vasculature: an experimental model for optic nerve neuropathy and trauma. *J Neurosci Methods.* 1996;70:21–25.
35. Lazarov-Spiegler O, Solomon AS, Schwartz M. Link between optic nerve regrowth failure and macrophage stimulation in mammals. *Vision Res.* 1999;39:169–175.
36. Isenmann S, Engel S, Gillardon F, et al. Bax antisense oligonucleotides reduce axotomy-induced retinal ganglion cell death in vivo by reduction of Bax protein expression. *Cell Death Differ.* 1999;6:673–682.
37. Rieger J, Wick W, Weller M. Human malignant glioma cells express semaphorins and their receptors, neuropilins and plexins. *Glia.* 2003;42:379–389.
38. Montolio M, Messeguer J, Masip I, et al. A semaphorin 3A inhibitor blocks axonal chemorepulsion and enhances axon regeneration. *Chem Biol.* 2009;16:691–701.
39. Corredor M, Bonet R, Moure A, et al. Cationic Peptides and Peptidomimetics Bind Glycosaminoglycans as Potential Sema3A Pathway Inhibitors. *Biophys J.* 2016;110:1291–1303.
40. Nitzan A, Kermer P, Shirvan A, et al. Examination of cellular and molecular events associated with optic nerve axotomy. *Glia.* 2006;54:545–556.
41. Kolodkin AL, Matthes DJ, Goodman CS. The semaphorin genes encode a family of transmembrane and secreted growth cone guidance molecules. *Cell.* 1993;75:1389–1399.
42. Kaneko S, Iwanami A, Nakamura M, et al. A selective Sema3A inhibitor enhances regenerative responses and functional recovery of the injured spinal cord. *Nat Med.* 2006;12:1380–1389.
43. He Z, Tessier-Lavigne M. Neuropilin is a receptor for the axonal chemorepellent Semaphorin III. *Cell.* 1997;90:739–751.
44. Rohm B, Ottemeyer A, Lohrum M, et al. Plexin/neuropilin complexes mediate repulsion by the axonal guidance signal semaphorin 3A. *Mech Dev.* 2000;93:95–104.
45. Sabag AD, Smolkin T, Mumblat Y, et al. The role of the plexin-A2 receptor in Sema3A and Sema3B signal transduction. *J Cell Sci.* 2014;127:5240–5252.
46. Nasarre C, Koncina E, Labourdette G, et al. Neuropilin-2 acts as a modulator of Sema3A-dependent glioma cell migration. *Cell Adh Migr.* 2009;3:383–389.